DOI 10.1007/s11015-021-01102-3
Metallurgist, Vol. 64, Nos. 11-12, March, 2021 (Russian Original Nos. 11-12, November–December, 2020)

SPECIFICS OF STRUCTURE FORMATION AND PROPERTIES OF WELDED JOINTS OBTAINED BY LASER-HYBRID WELDING OF LONGITUDINAL PIPE JOINTS

L. A. Efimenko,[1] O. E. Kapustin,[2] D. V. Ponomarenko,[3] I. Yu. Utkin,[4] M. A. Fedorov,[5] and A. I. Romantsov[6]

UDC 621.791.753.5

The authors have studied the microstructure and properties of the welded joints obtained by laser-hybrid welding (LHW) in combination with submerged multi-arc welding (SMAW) and by the classical method. The potential of using a LHW/SMAW combination were demonstrated in an attempt to increase the resistance of welded joints to brittle fracture, provide uniform structural and phase composition of the weld and heat affected zone (HAZ), and ensure that the strength and plastic properties of the welded joints are consistent with the corresponding parameters of the base metal.

Keywords: laser-hybrid welding, near-weld area of the heat affected zone, mechanical properties, microstructure.

Currently, an increase in productivity of gas supply is associated with higher operating pressures for pumping gas, which requires the use of thick-walled pipes made of grade X70 and higher. Grade X70 is a fairly common grade of steel used for high-pressure pipe applications, and the main technological operation is submerged multi-arc welding (SMAW), which utilizes several arcs (from three to five) in a single weld pool [1–3]. The main disadvantage of the SMAW technology is high heat input into the welded metal, which contributes to altering the performance parameters of the welded joints, sometimes rendering them inconsistent with the regulatory requirements [1, 4, 5]. This issue becomes especially critical when it comes to welding thick-walled pipes with a wall thickness of 20 mm and more. Welding of such pipes results in the formation of an extensive heat affected zone (HAZ), which demonstrates low mechanical characteristics compared to the base pipe metal and weld metal. Therefore, a search for alternative welding processes that would allow solving technical problems arising during the production of high-pressure pipes is very important.

This paper analyzes the possibility of combining a laser-arc power source (LHW) and a submerged multi-arc welding (SMAW) of the longitudinal joints of high-pressure pipes, which would enable high efficiency of the welding process, while providing the required set of mechanical properties.

The study was conducted using welded joints of the 21.6 mm thick plates made of grade X70 steel having the following chemical composition, wt.%: C — 0.078, Mn — 1.48, Si — 0.28, Ni — 0.21, Cr — 0.13, Al — 0.024, Nb — 0.03, Ti — 0.013, V < 0.002. In this case, two technological processes were implemented, which are applicable to welding longitudinal pipe joints (Fig. 1).

[1] Gubkin Russian State University of Oil and Gas (National Research University), Moscow, Russia; e-mail: lefimen@yandex.ru.
[2] Gubkin Russian State University of Oil and Gas (National Research University), Moscow, Russia; e-mail: svarka@gubkin.ru.
[3] Gubkin Russian State University of Oil and Gas (National Research University), Moscow, Russia; e-mail: dariaponomarenko@mail.ru.
[4] Gubkin Russian State University of Oil and Gas (National Research University), Moscow, Russia; e-mail: iutkin89@ya.ru.
[5] PJSC "Chelyabinsk Pipe Rolling Plant," Chelyabinsk, Russia; e-mail: mikhail.fedorov@chelpipe.ru.
[6] PJSC "Chelyabinsk Pipe Rolling Plant," Chelyabinsk, Russia; e-mail: Aleksandr.Romantsov@chelpipe.ru.

Translated from Metallurg, Vol. 64, No. 11, pp. 63–68, November, 2020. Original article submitted March 16, 2020.

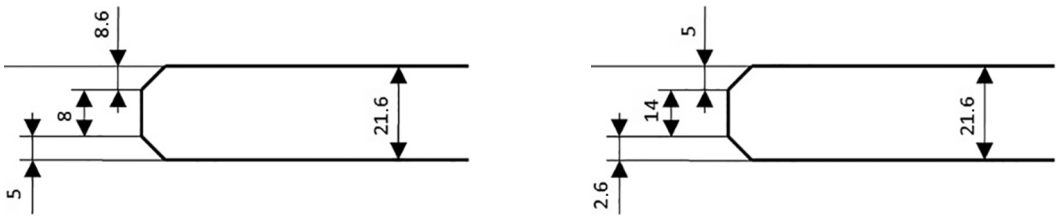

Fig. 1. Edge preparation for SMAW (a) and LHW (b).

Table 1
Classical Submerged Multi-Arc Welding of Longitudinal Joints and Cap Welds When Implementing a Laser-Hybrid Welding Technology

Current, A					Voltage, V					Welding rate, cm/min	Heat input, kJ/cm
1	2	3	4	5	1	2	3	4	5		
SMAW conditions for inner welds											
900	800	700	650	–	33	35	37	40	–	165	39.9
SMAW conditions for outer welds											
1200	950	850	800	700	33	35	37	39	41	195	50.5
Cap weld conditions when implementing a LHW for inner welds											
400	380	350	–	–	32	34	36	–	–	167	13.8
Cap weld conditions when implementing a LHW for outer welds											
400	380	350	–	–	32	35	38	–	–	100	23.6

A classical option (submerged multi-arc welding) was intended to complete an inner weld using four arcs and an outer weld using five arcs in a single weld pool. In this case, the weld heat input was about 40 kJ/cm and 50 kJ/cm for inner and outer welds, respectively (Table 1).

By recording the thermal welding cycles (SMAW) according to the procedure described in Ref. [6], it was established that the cooling rate of the metal in the near-weld area of the heat affected zone (HAZ) in the temperature range of austenitic decomposition by diffusion (w_{8-5}) was about 5 °C/s.

The second option was to weld the root face using the laser-hybrid technology with subsequent application of cap welds by a submerged multi-arc welding at a number of arcs reduced down to three (see Table 1). As can be seen, as a result of reduction in the number of welding wires simultaneously supplied to the weld pool at a decreased current, the formation of both inner and outer welds was carried out at a significantly lower heat input.

Based on the results of analysis of the thermal cycle parameters, it was determined that during root-face welding by using the laser-hybrid technology, the cooling rate was about 150 °C/s. In the process of subsequent cap weld application, this section was heated to temperatures in excess of Ac_3 and cooled at the cooling rates of about 30 and 18 °C/s when applying the inner and outer cap welds, respectively.

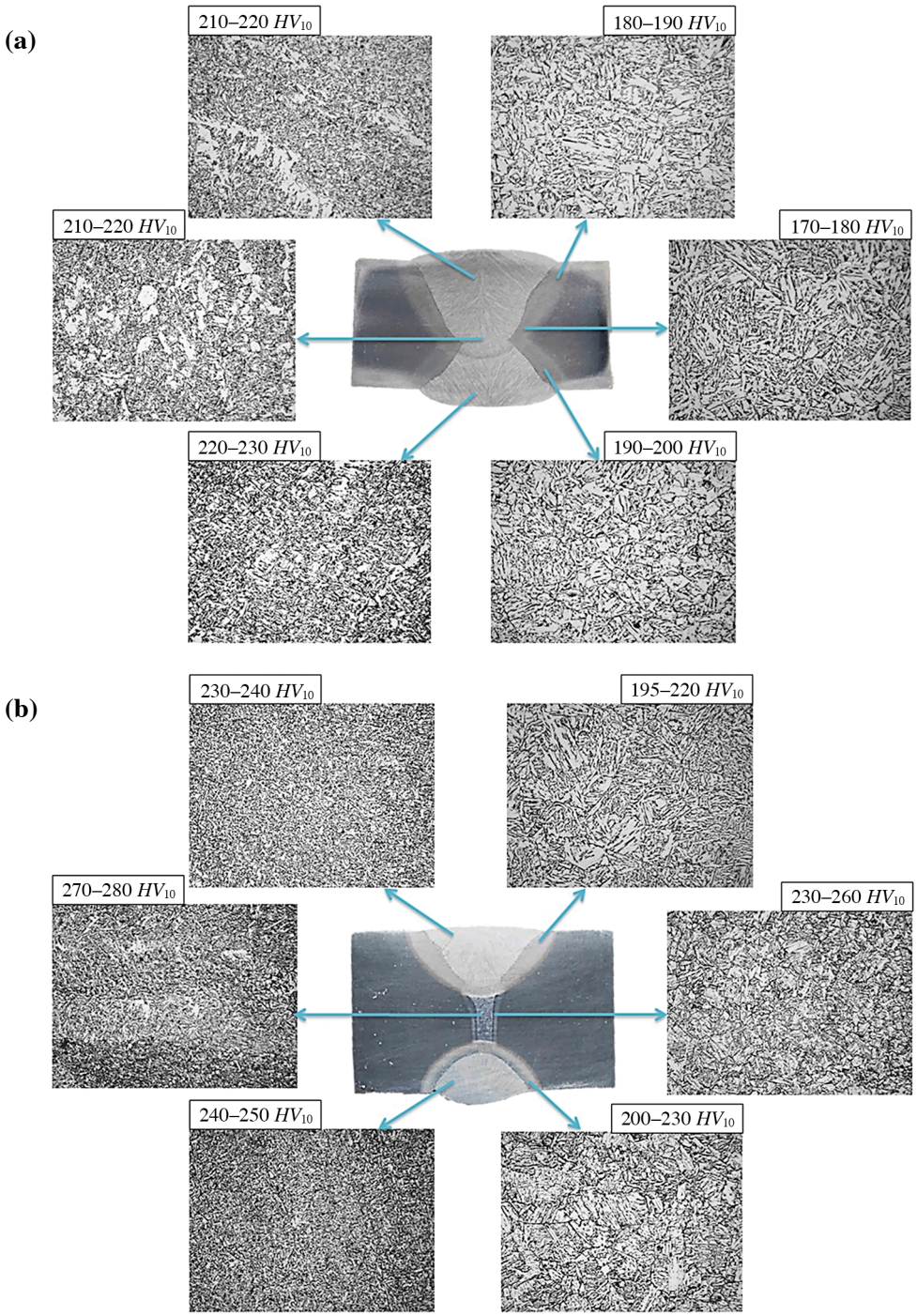

Fig. 2. Macro- and microstructures of welded joints obtained by SMAW (a) and LHW/SMAW combination (b), × 500.

Figure 2 shows the macro- and microstructures of the welded joints produced according to the analyzed welding options. Figure 3 shows the structural diagram of the metal in the near-weld area of the heat affected zone (HAZ). As can be seen from the macrostructures, the use of the LHW/SMAW combination made it possible to significantly reduce the HAZ width compared to its value in case of a classical SMAW. Specifically, in the central (thickness-wise) part of the welded joint, such width decreased from 3,700–3,800 to 590–600 μm.

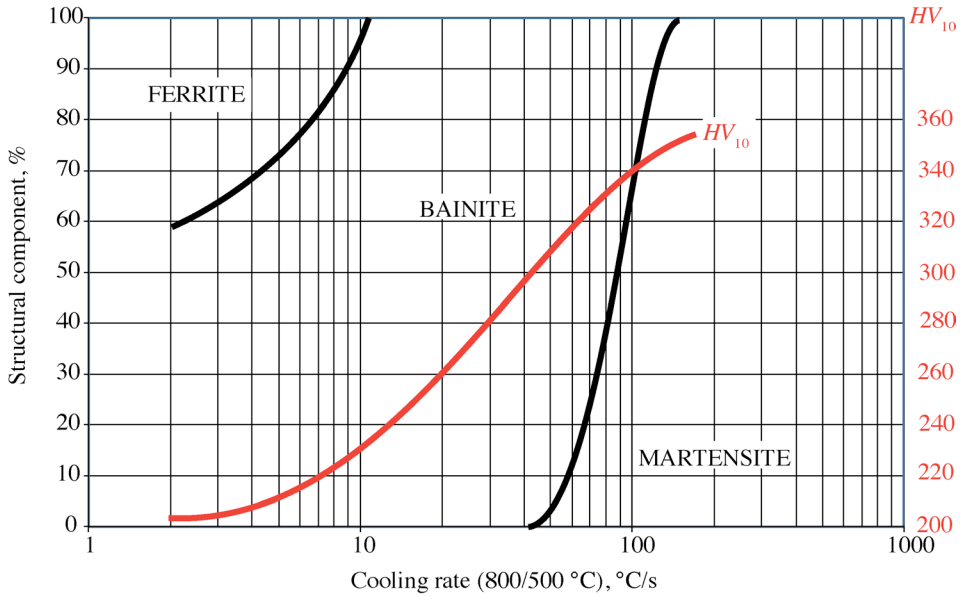

Fig. 3. Structural diagram of the near-weld area of the heat affected zone of grade X70 steel.

By analyzing the structural and phase compositions of the welded joints (Fig. 2 (a)), it was shown that during classical SMAW, a ferrite-bainite structure is formed in the weld and HAZ metal. The ferrite phase content of the upper weld and its HAZ does not exceed 25%. Metal hardness is 210 to 220 *HV*. The lower weld and its HAZ contain about 15 to 20% of ferrite. The hardness of the weld metal is 220 to 230 *HV*. In the overlap area, the structure of the weld metal and HAZ is closer to the corresponding sections of the upper weld and its HAZ.

As a result of exposure to the LHW process, austenitic decomposition in the weld metal and HAZ mainly occurs in the martensitic region (see Fig. 3), while the hardness of the weld metal and HAZ is about 350 to 360 *HV*. A subsequent heating of the metal of the laser exposure zone with the heat, generated during the formation of both inner and outer cap welds, contributes to a recrystallization of the martensitic phase and formation of predominantly homogeneous bainite phase structure. In this case, the hardness of the weld metal and HAZ of the weld joint produced by a laser-hybrid welding is reduced to 270–280 and 230–260 *HV*, respectively (see Fig. 2 (b)).

In addition to hardness measurement, properties of the welded joints were evaluated under the static and dynamic loading conditions.

Static tension tests were performed using type III samples according to GOST 6996 [7]. A ten-tone tensile tester (LFMZ-100) was used. The obtained strength and plastic characteristics are shown in Table 2. It should be noted that during static tension test, all samples failed along the base metal regardless of the utilized welding technology. No significant differences were observed between the mechanical characteristics.

The brittle fracture resistance was evaluated based on the impact bending test results using type IX samples (Charpy) measuring $10 \times 10 \times 55$ mm in accordance with GOST 6996. This parameter was given a special consideration, since it is structurally sensitive and changes the most during welding [8–11]. The tests were conducted using a motorized pendulum impact tester (INSTRON MPX-450) at minus 40°C. The samples were cut out from the central section along the thickness of the cross-section. When evaluating the impact toughness of the weld metal, the notch was applied in the center for both welding methods. In case of the samples used to estimate the impact toughness values in the near-weld area of the heat affected zone of the welded joints obtained by SMAW, the notch was applied in accordance with the recommendations provided in Ref. [12]. Moreover,

Table 2
Strength and Plastic Characteristics of Welded Joints (min–max/avr)

Welding technology	Ultimate strength σ_u, MPa	Yield point σ_y, MPa	Percent elongation δ, %	Percent reduction ψ, %
Classical submerged multi-arc welding	(608–610)/**609**	(497–514)/**505**	(20–23)/**22**	(69–76)/**73**
Laser-hybrid welding with subsequent cap weld application	(617–627)/**622**	(507–515)/**511**	(18–21)/**20**	(60–70)/**65**

Table 3
Impact Toughness of the Weld Joint and Weld Junction Metal

Welding technology (notch location)	KCV^{-40}, J/cm^2 (min–max/avr)
Classical submerged multi-arc welding:	
welded joint	(65–157)/106
weld-fusion line	(54–150)/106
Laser-hybrid welding with subsequent cap weld application:	
welded joint	(201–270)/241
weld-fusion line	(210–260)/227

due to the curvature of the weld-fusion line, the impact toughness values were partially determined by the contribution of the corresponding property of the weld metal. In case of LHW, the notch was applied along an essentially straight weld-fusion line. The micromechanism of fracture was studied based on the fractographic images of the fracture surface of the samples obtained using a scanning electron microscope (Phenom Pro X).

The analysis of the shock bending test results (Table 3) has shown that welded joints obtained by the SMAW method have lower impact toughness values for both weld metal and near-weld area of the heat affected zone compared to the corresponding welded joint areas obtained using the LHW technology. The average value of the KCV^{-40} parameter is equal to 106 J/cm^2 for both the weld metal and the near-weld area of the heat affected zone. It is important to note a large gap between the minimum and maximum impact toughness values. This points to the fact that the welded joints operate in the viscous-brittle transition zone. In this case, the minimum impact toughness values are close to the lower allowable level [5].

A study of the fractographic images of the fracture surfaces of the samples used to estimate the impact toughness of the welded joints produced by the SMAW method (Fig. 4) has shown that the majority of the fracture surface demonstrates relatively flat crystallographic facets (see Fig. 4 (a)), much like the facets of a transgranular cleavage.

The fracture surfaces of the samples having the KCV^{-40} values of the order of 157 J/cm^2 mainly consist of viscous component (see Fig. 4 (b)).

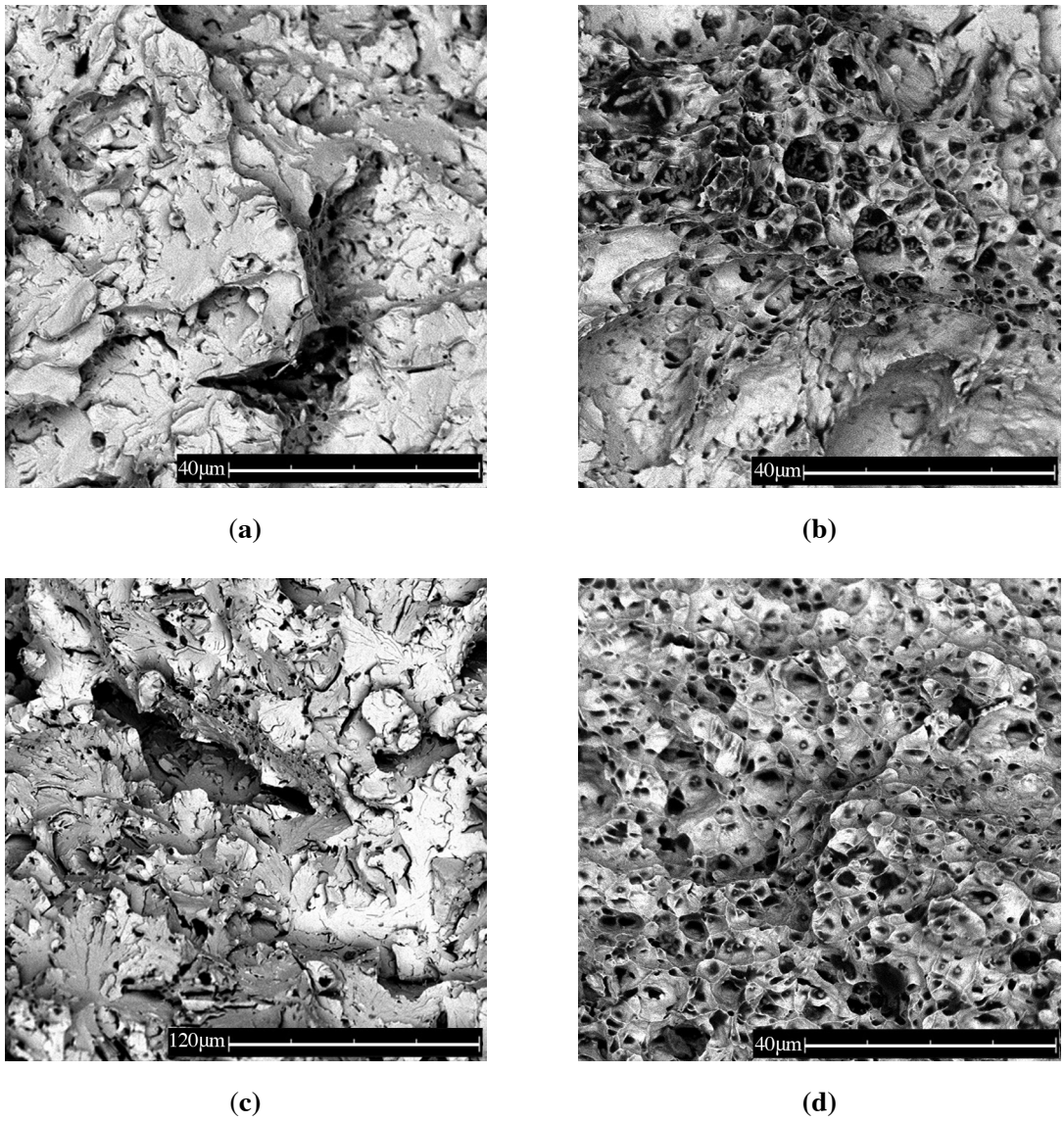

Fig. 4. Fractographic images of the weld metal fractures (a), (b) and near-weld area of the heat affected zone (c), (d) of the welded joint obtained by SMAW.

A similar fracture mechanism is also seen in case of the surfaces of the samples used to estimate the impact toughness of the near-weld area of the heat affected zone (see Fig. 4 (b, d)).

The welded joints obtained using the laser-hybrid welding technology are characterized by close and higher values of impact toughness compared to the welds produced by the classical method (see Table 3). Specifically, the KCV^{-40} values vary from 201 to 270 J/cm^2 for the weld metal and from 210 to 260 J/cm^2 for the near-weld area of the heat affected zone.

The micromechanism of the fracture surface of the metal of the specified welded joint areas is represented by the quasi-spalling facets and the presence of a large number of viscous metal links between them having a dimpled structure (Fig. 5). The peripheral sections of the quasi-spalling facets have smooth outlines, pointing to a noticeable plastic deformation of these metal volumes. Such structure of the fractures provides higher impact toughness values.

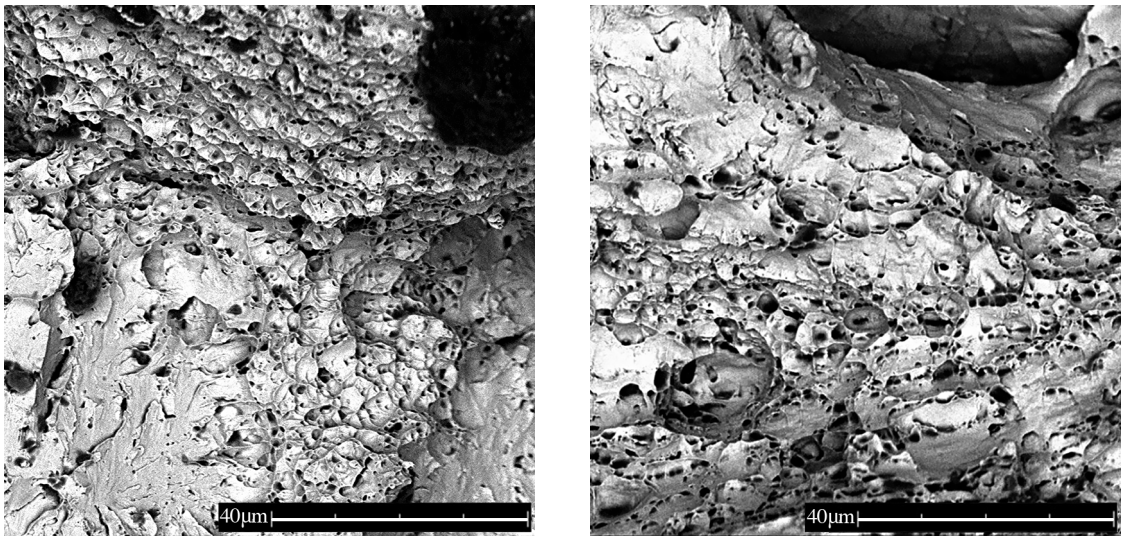

(a) **(b)**

Fig. 5. Fractographic image of the weld metal fractures (a) and near-weld area of the heat affected zone (b) of the welded joint obtained by LHW with subsequent cap weld application, × 3,000.

Thus, by using a combination of laser-hybrid root-face welding technology and submerged multi-arc welding of the cap welds, it became possible to ensure a higher welded joint resistance to brittle fracture compared to the corresponding parameter of the welded joints obtained by the classical submerged multi-arc welding.

Conclusions

Compared to the classical welding, the use of the laser-hybrid welding technology with subsequent completion of the cap welds by the automatic submerged multi-arc welding makes it possible to:

- ensure a more uniform structural and phase composition of the weld metal and HAZ;
- obtain strength and plastic properties of the welded joints, which are not lower than the corresponding parameters of the base metal;

and

- provide higher resistance to brittle fracture (higher impact toughness values and a rather energy-intensive micromechanism of fracture).

REFERENCES

1. A. A. Rybakov, T. N. Filipchuk, and V. A. Kostin, "Specifics of microstructure and impact toughness of the weld metal of pipes made of high-strength steel with niobium and molybdenum," *Avtomaticheskaya Svarka*, Nos. 3-4, 17–24 (2015).
2. N. Ochi, S. Okano, M. Mochizuki, J. Shimamura, and N. Ishikawa, "Thermal conduction theoretical analysis of temperature distribution during multiple-electrode submerged arc welding," *Welding International*, **28**, 3, 174–183 (2014).
3. A. N. Bortsov, I. P. Shabalov, A. A. Velichko, K. Yu. Mentyukov, and I. Yu. Utkin, "Specifics of multi-electrode submerged welding in high-strength pipe production," *Metallurg*, No. 4, 69–76 (2015).

4. L. A. Yefimenko, T. S. Yesiev, D. V. Ponomarenko, S. P. Sevastyanov, and I. Yu. Utkin, "Effect of thermal treatment on impact toughness of the weld metal of pipes obtained by a submerged multi-arc welding," *Metallurg*, No. 3, 59–63 (2018).
5. STO Gazprom 2–4.1–713–2013, *Technical Specification for Pipes and Fittings: Organization Standard* [in Russian] (replaces STO Gazprom 2–4.1–273–2008), introduced on February 11, 2013; OAO Gazprom, Moscow (2014).
6. L. A. Yefimenko, A. P. Derkach, O. Ye. Kapustin, and S. P. Sevostyanov, "Justification of the selection of a calculation scheme for determining a thermal cycle parameter of submerged multi-arc welding," *Svarka i Diagnostika*, No. 6, 26–27 (2017).
7. GOST 6996–66, *Welded Joints. Methods for Determining Mechanical Properties* [in Russian].
8. L. Lan, X. Kong, C. Qiu, and D. Zhao, "Influence of microstructural aspects on impact toughness of multi-pass submerged arc welded HSLA steel joints," *Materials & Design*, **90**, 488–498 (2016).
9. M. Hamada, "Control of strength and toughness at the heat affected zone," *Welding International*, **17**, 4, 265–270 (2003).
10. Z. Li, X. Zhao, and D. Shan, "Impact toughness of subzones in the intercritical heat-affected zone of low-carbon bainitic steel," *Materials* (Basel), **11**, 6, 959 (2018).
11. G. A. Filippov, "Mechanisms of metal fracture in high-strength steel pipes and methods of improving ductile and brittle fracture resistance," *Int. Conf. Proc. "Manufacture, testing and practical use of grade X80/X90 large-diameter pipes,"* Moscow, April 6–8 (2011), pp. 101–114.
12. *Offshore Standard DNV-OS-F101, Submarine Pipeline Systems* [in Russian], Inf. Rekl. Tsentr Gaz. Prom., Moscow (2006).